Mid-infrared dual-comb spectroscopy with an optical parametric oscillator

Zhaowei Zhang,[1,2,]* Tom Gardiner,[2] and Derryck T. Reid[1]

[1]Institute of Photonics and Quantum Sciences, Heriot-Watt University, Riccarton, Edinburgh EH14 4AS, UK

[2]National Physical Laboratory, Hampton Road, Teddington, London TW11 0LW, UK

*Corresponding author: z.zhang@hw.ac.uk

We present the first implementation of mid-infrared dual-comb spectroscopy with an optical parametric oscillator. Methane absorption spectroscopy was demonstrated with a resolution of 0.2 cm^{-1} (5 GHz) at an acquisition time of ~10.4 ms over a spectral coverage at 2900–3050 cm^{-1}. The average power from each individual mid-infrared comb line was ~1 μW, representing a power level much greater than typical difference-frequency-generation sources. Mid-infrared dual-comb spectroscopy opens up unique opportunities to perform broadband spectroscopic measurements with high resolution, high requisition rate, and high detection sensitivity. © 2013 Optical Society of America

OCIS codes: (300.6300) Spectroscopy, Fourier transforms; (300.6390) Spectroscopy, molecular; (120.6200) Spectrometers and spectroscopic instrumentation; (190.4970) Parametric oscillators and amplifiers.
http://dx.doi.org/10.1364/OL.38.003148

The mid-infrared (mid-IR) region, defined here as from 2.5 to 25 μm (4000 – 400 cm^{-1}), contains the fundamental rovibrational absorption bands of many molecules and is often referred to as the molecular fingerprint region. High-resolution spectroscopy in this region employs Fourier-transform infrared (FTIR) spectrometers as the tools of choice for the identification of molecular species, quantitative analysis of complex mixtures, the investigation of dynamic systems, biological and biomedical spectroscopy, microspectroscopy, and hyperspectral imaging [1]. Conventionally, mid-IR FTIR spectroscopy is conducted with a thermal light source (e.g., a Globar) and a spectrometer based on a Michelson interferometer containing a scanning mechanical delay line. However, the use of spatially incoherent thermal light sources limits the detection sensitivity of FTIR techniques and their applicability in free-space sensing or microspectroscopy due to their low spectral brightness and poor directionality. In addition, the acquisition rate and spectral resolution of traditional FTIR spectrometers are limited, respectively, by the velocity and displacement of the scanning mechanical delay line used in these systems.

Mode-locked lasers are broadband optical sources possessing exceptional spatial coherence, and when configured in the mid-IR region they have been shown to be promising sources for FTIR spectroscopy [2]. Such laser sources inherently support high detection sensitivity, are compatible with the use of multipass cells for trace gas sensing, and enable long-range open-path sensing and FTIR microspectroscopy. In the frequency domain, adjacent longitudinal cavity modes of a mode-locked laser are separated by a precise interval in both frequency and phase, forming a frequency comb. In a dual-comb spectrometer, two laser frequency combs with slightly different comb-line spacings (or pulse repetition rates, f_{rep}) and stabilized carrier-envelope-offset (CEO) frequencies (f_{CEO}) are heterodyned after passing through a sample, yielding a down-converted radio-frequency (RF) comb encoding information about the absorption experienced by the combs [3–11]. This RF comb manifests itself as an interferogram, analogous to that obtained using a mechanically scanning Michelson FTIR spectrometer, but the absence of moving parts in a dual-comb spectrometer overcomes the speed and resolution limitations of its conventional counterpart. The resolution is only limited by the comb-line interval (the pulse repetition frequency), and the recording time is the inverse of the difference in the pulse repetition frequencies.

Until now, only a limited number of dual-comb spectroscopy experiments were conducted in the mid-IR region, and all such systems were implemented with low-efficiency and low-power difference frequency generation frequency combs [3,4,8]. Recently, we introduced a new dual-comb source comprising a single synchronously pumped optical parametric oscillator (OPO) driven by two independent lasers [12,13] and capable of producing two asynchronous—but otherwise identical—mid-IR pulse sequences. Here, we describe the first application of this system to mid-IR dual-comb spectroscopy, from which high-resolution absorption spectra of methane were obtained in the spectral range of 2900–3050 cm^{-1} with an acquisition rate of 96 Hz.

The asynchronous mid-IR comb sources were based on the scheme detailed in [13]. Two independent pump sources of identical design and performance, but slightly different repetition rates, were combined on a 50:50 dielectric beam splitter. Each source was composed of a fiber amplifier seeded by a mode-locked Yb:KYW laser. The average power, center wavelength, 3 dB spectral bandwidth, and pulse width of each pump source were 2.5 W, 1058 nm, 18 nm (4.82 THz), and ~3 ps, respectively. The output from the beam splitter was used to pump an OPO incorporating a 20 mm long magnesium oxide-doped periodically poled lithium niobate (MgO:PPLN) crystal, generating two idler channels of broadband mid-IR pulses. The high group-delay dispersion of the OPO cavity, mainly contributed by the MgO:PPLN crystal, made it possible for two optical pulse sequences of nearly identical wavelengths but with different repetition rates to be resonant simultaneously [13]. These asynchronous mid-IR pulse sequences left the OPO through a
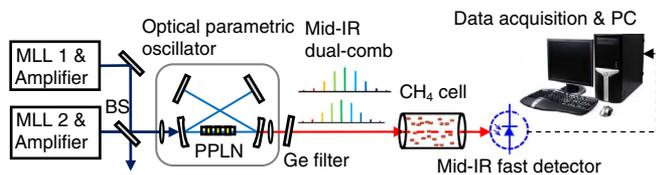
Fig. 1. Layout of the mid-IR dual-comb spectrometer. MLL, mode-locked laser; BS, beam splitter; PPLN, periodically poled lithium niobate.

curved resonator mirror and possessed excellent spatial overlap. The average power, center wavelength, –3 dB spectral bandwidth and pulse width of each mid-IR idler channel were 100 mW, 3313 nm, 172 nm (4.70 THz), and ~3 ps respectively. The pulses from both idler channels were strongly chirped, with a duration-bandwidth product of 14.

The layout of the mid-IR dual-comb spectrometer is shown in Fig. 1. The repetition frequency of one channel was stabilized to a 100 MHz RF reference source, while the repetition-frequency difference (Δf) between the two channels was free-running at 96 Hz (unlocked). The CEO frequencies of both channels were also free-running. The asynchronous mid-IR pulse sequences passed through a 20 cm cell, containing a 1 atm mixture of nitrogen with a low concentration (~0.7%) of methane. The signal was detected by a thermoelectrically cooled MCZT (HgCdZnTe) photovoltaic detector with a bandwidth of 100 MHz. In the time domain, one mid-IR pulse sequence is sampled by the other with a slightly different pulse repetition rate, at a sampling interval of $\Delta f/f_{rep}^2$, forming a time-domain interferogram. In the frequency domain, the laser frequency lines from the two asynchronous combs heterodyne with each other, generating an RF comb with a comb spacing of Δf. After Nyquist filtering by a 50 MHz low-pass filter, the time-domain signal was sampled by a high-resolution 14 bit data acquisition card with a 50 MHz bandwidth at a sampling rate of 100 MSamples/s.

The detected time-domain interferogram is shown in Fig. 2. The intense spikes are the interferograms corresponding to the temporal overlap of two pulses, and these repeat with a period of 10.4 ms ($1/\Delta f$). One of the mode-locked Yb:KYW seed lasers was running in a double-pulse mode, and this behavior was transferred to the mid-IR pulse sequence in the OPO. Thus, the interferogram shows two bursts in each period, with two series of bursts with a period of 10.4 ms and separated from each other by 5.8 ms. A Fourier transform was
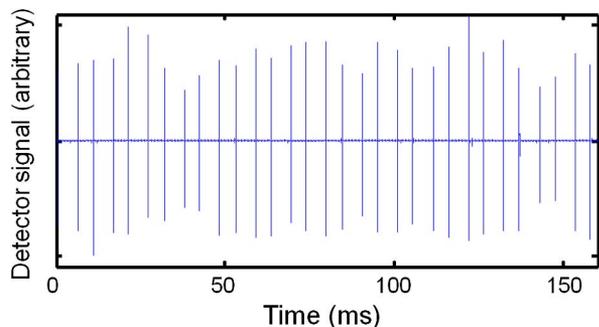

Fig. 2. Time-domain interferogram ($\Delta f = 96$ Hz). One of the mid-IR pulse sequences operated in a double-pulse mode.
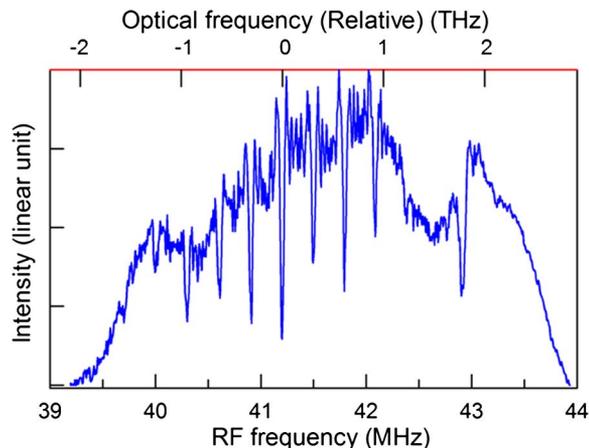

Fig. 3. Fourier-transform spectrum expressed in the RF (lower axis) and optical (upper axis) domains.

performed over a single interferogram to reveal the RF comb (the lower axis in Fig. 3), which was scaled to the optical domain with a scaling factor of $f_{rep}/\Delta f = 1.04 \times 10^6$, as shown by the upper axis in Fig. 3. We implemented a 0.2 ms time window over the interferogram, so the transformed spectrum shown in Fig. 2 had a resolution of 5 kHz for the RF spectrum and 5 GHz (0.2 cm^{-1}) for the optical spectrum. Spectra with much higher resolution but lower signal-to-noise ratio (SNR) could be achieved from the same interferogram by use of a broader time window.

Shown in Fig. 4 are normalized optical spectra, obtained from four single measurements, and a spectrum obtained by averaging over eight measurements. It is clear that useful spectroscopic data are accessible from just a single interferogram, but also that the SNR can be improved significantly by averaging. It is noteworthy that the acquisition rate was 96 Hz; an individual measurement was completed within a time duration of
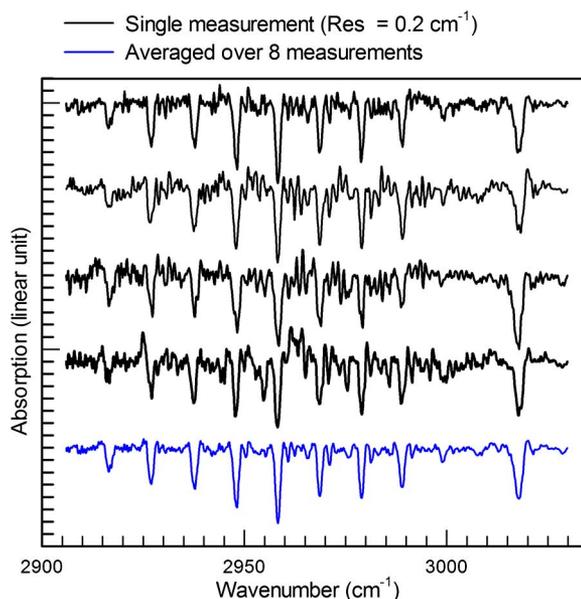

Fig. 4. Normalized methane absorption spectra for single measurements (top 4 traces, black) and an averaged spectrum (bottom trace, blue).
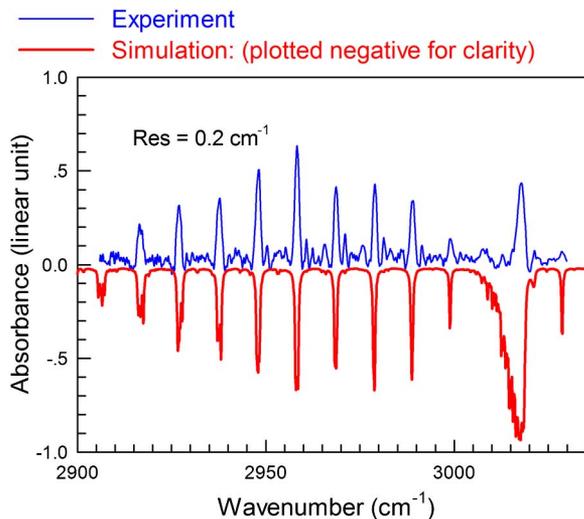
Fig. 5. Comparison between the measured and simulated absorption spectrum (fitting parameters: 0.65% methane at 1 atm; 20 cm cell; resolution = 0.2 cm^{-1}).

10.4 ms, and within 1 min, 5760 measurements could be conducted, implying a potential enhancement of 75 times in the spectral SNR over a single measurement [1]. In this experiment, since the CEO frequencies of the dual mid-IR combs were neither stabilized or monitored in real time, information about the absolute optical frequency was not directly available from the Fourier transform. Rather, we obtained the absolute optical frequency by aligning the frequencies in the Q branch of the methane absorption spectrum to the known value at 3317 cm^{-1}. Another option to determine the absolute optical frequency is by using passive optical filters with known central frequencies as frequency references [14].

Shown in Fig. 5 is a comparison between the measured methane absorption spectrum (averaged over eight interferograms) and the simulated spectrum, based on the HITRAN database and a methane concentration of 0.65% at 1 atm with a resolution of 0.2 cm^{-1}. The agreement between the experimental and simulated spectra is excellent for the P branch, while we believe the discrepancy in the Q branch is due to experimental uncertainties in the normalization procedure we used.

Dual-comb spectroscopy can be understood as a form of multiheterodyne spectroscopy in which the beat between laser-frequency comb 1 ($f_1 = f_{CEO,1} + n_1 n_{rep,1}$) and laser-frequency comb 2 ($f_2 = f_{CEO,2} + n_2 f_{rep,2}$) generates a downshifted RF comb $f = f_1 - f_2 = \delta + N\Delta f$, where $\delta = f_{CEO,1} - f_{CEO,2}$ represents the difference between the CEO frequencies of the two channels. To fully exploit the potential of mid-IR dual-comb spectroscopy, δ must be stabilized [5,8] or monitored [7,10,11], thus enabling precise determination of the absolute optical frequency, ensuring high spectral resolution for resolving

each individual comb tooth and facilitating higher SNR through the application of intensive coherent averaging. In this work, δ was free-running; however, the accurate alignment between the P-branch spectrum and simulated data implies that δ was passively stable during the 0.2 ms interferogram window. Further work to implement a dual-comb spectroscopy measurement with a fully stabilized system [15] is in progress.

In summary, we have reported the first dual-comb asynchronous spectroscopy with an OPO operating in the important mid-IR molecular fingerprinting region. The average power of the individual mid-IR comb line was approximately 1 μW, representing a huge improvement over previously reported mid-IR dual-comb systems. These initial results demonstrate the benefits and practicality of mid-IR dual-comb OPO spectroscopy in terms of scanning speed, resolution, SNR, and spectral coverage.

References
1. P. R. Griffiths and J. A. De Haseth, *Fourier Transform Infrared Spectrometry* (Wiley, 2007).
2. K. A. Tillman, R. R. J. Maier, D. T. Reid, and E. D. McNaghten, Appl. Phys. Lett. **85**, 3366 (2004).
3. F. Keilmann, C. Gohle, and R. Holzwarth, Opt. Lett. **29**, 1542 (2004).
4. A. Schliesser, M. Brehm, F. Keilmann, and D. van der Weide, Opt. Express **13**, 9029 (2005).
5. I. Coddington, W. C. Swann, and N. R. Newbury, Phys. Rev. Lett. **100**, 013902 (2008).
6. B. Bernhardt, E. Sorokin, P. Jacquet, R. Thon, T. Becker, I. T. Sorokina, N. Picqué, and T. W. Hänsch, Appl. Phys. B **100**, 3 (2010).
7. J.-D. Deschenes, P. Giaccarri, and J. Genest, Opt. Express **18**, 23358 (2010).
8. E. Baumann, F. R. Giorgetta, W. C. Swann, A. M. Zolot, I. Coddington, and N. R. Newbury, Phys. Rev. A **84**, 062513 (2011).
9. A. Schliesser, N. Picqué, and T. W. Hänsch, Nat. Photonics **6**, 440 (2012).
10. T. Ideguchi, A. Poisson, G. Guelachvili, N. Picqué, and T. W. Hänsch, arXiv:1201.4177 (2012) (to be published).
11. T. Ideguchi, A. Poisson, G. Guelachvili, T. W. Hänsch, and N. Picqué, Opt. Lett. **37**, 4847 (2012).
12. Z. Zhang, J. Sun, T. Gardiner, and D. T. Reid, Opt. Express **19**, 17127 (2011).
13. Z. Zhang, C. Gu, J. Sun, C. Wang, T. Gardiner, and D. T. Reid, Opt. Lett. **37**, 187 (2012).
14. P. Giaccari, J.-D. Deschênes, P. Saucier, J. Genest, and P. Tremblay, Opt. Express **16**, 4347 (2008).
15. Z. Zhang, X. Fang, T. Gardiner, and D. T. Reid, Opt. Lett. **38**, 2077 (2013).